npj | precision oncology

Brief communication

Published in partnership with The Hormel Institute, University of Minnesota

https://doi.org/10.1038/s41698-026-01274-8

Clonal determinants of organotropism and survival in metastatic uveal melanoma

Bailey S. C. L. Jones[1], Emma Hammes[2], Patrick C. Demkowicz[3], Mitchelle Matesva[3], Renelle Pointdujour-Lim[1,4], John H. Sinard[1,2], Antonietta Bacchiocchi[4], Ruth Halaban[4], Marcus Bosenberg[2,5], Mario Sznol[5,6], Harriet M. Kluger[5,6] & Mathieu F. Bakhoum[1,2,5] ✉

Uveal melanoma (UM), the most common intraocular cancer in adults, metastasizes to the liver in 90% of cases. Integrating DNA sequencing of 144 metastases with decade-long patient outcomes, we found that liver metastases are more enriched for *BAP1*-mutant, monosomy 3 clones, compared to extrahepatic metastases. *BAP1* loss in liver metastases independently predicts poorer post-metastatic survival. Patterns of dissemination are set early in primary tumors, enabling molecular profiling to forecast metastatic spread.

Metastasis, the process by which cancer cells spread to distant organs, is influenced by the interplay between cancer cells and their target organ microenvironments. This phenomenon, known as organotropism, has been observed in various malignancies, including uveal melanoma (UM), the most common intraocular cancer in adults[1–3]. The majority (90%) of patients that develop UM metastases have liver involvement, establishing UM as an excellent model for studying organotropism in cancer[4,5]. Notably, patients with UM metastases involving the liver experience significantly worse survival outcomes than those with only extrahepatic metastases, underscoring the need to clarify the molecular drivers of hepatic tropism[6]. While *BAP1* and monosomy 3 are markers for poor in primary tumors, whether they preferentially promote liver-specific dissemination—and how they influence outcomes after metastasis—is unknown.

To determine tumor-intrinsic drivers of organotropism, we compared hallmark mutations in hepatic versus extrahepatic UM metastases using whole-exome and genome sequencing data (please see "Methods" for details). The resulting patterns show that metastatic spread in UM is not random but dictated by defined clones present in the primary tumor. Consequently, applying this molecular classification to an independent primary tumor cohort with long-term follow-up accurately predicted patterns of metastatic spread, validating primary-tumor profiling as a tool to predict patterns of metastatic dissemination.

Results

Mutational landscape and mutual exclusivity in primary and metastatic UM

We first examined the distribution of hallmark UM mutations in metastasis. In primary UMs, there are two clusters of genes with recurring mutations[7]. The first cluster includes the mutually exclusive *GNAQ* and *GNA11*, which are implicated in UM tumorigenesis[7]. The second cluster includes mutations in *BAP1*, *EIF1AX*, and *SF3B1*, which provide prognostic information and exhibit a general pattern of mutual exclusivity[7–9]. In The Cancer Genome Atlas (TCGA)[9], there were 34 primary UM samples with only *GNAQ* mutations, 38 with only *GNA11* mutations, and 2 with both, yielding a Jaccard index of 0.03 indicating a high degree of mutual exclusivity (p <0.0001). In the second cluster of genes, there were 12 primary samples with only *BAP1* mutations, 16 with only *SF3B1*, 9 with only *EIF1AX*, 1 with both *BAP1* and *SF3B1* (Jaccard index 0.03, $p = 0.2778$), and 1 with both *SF3B1* and *EIF1AX* mutations (Jaccard index 0.04, $p = 0.4421$) (Fig. 1a, b). We analyzed the distribution of these mutations in metastases within a cohort of 144 metastatic UMs procured at our institution and from published cohorts (Sources in Table 1)[10–13]. There were 61 and 69 samples with *GNAQ* and *GNA11* mutations, respectively. In the second cluster of genes, there were 77 samples with only *BAP1* mutations, 28 with only *SF3B1*, 7 with only *EIF1AX*, 6 with both *BAP1* and *SF3B1* (Jaccard index 0.05, p <0.0001), and 3 with both *BAP1* and *EIF1AX* mutations (Jaccard index 0.03, $p = 0.0062$) (Fig. 1a, b). While we observe statistically significant independent distribution between *GNAQ/11* mutations in primary and metastatic specimens, we observe statistical significance between *BAP1/SF3B1* and *SF3B1* in metastatic but not primary tumors. Given the smaller sample availability of *BAP1/EIF1AX/SF3B1* mutational profiling of primary tumors, further analysis of additional specimens is warranted. Taken together, these mutation patterns indicate that mutually exclusive distributions in primary UMs are largely preserved in metastatic lesions, such that the mutually exclusive pattern within the two layers of mutations, (1) *GNAQ/GNA11* and (2) *BAP1/EIF1AX/SF3B1*, is evidenced in both primary and metastatic UMs.

[1]Department of Ophthalmology & Visual Science, Yale School of Medicine, New Haven, CT, USA. [2]Department of Pathology, Yale School of Medicine, New Haven, CT, USA. [3]Yale School of Medicine, New Haven, CT, USA. [4]Department of Dermatology, Yale School of Medicine, New Haven, CT, USA. [5]Yale Cancer Center, Yale School of Medicine, New Haven, CT, USA. [6]Department of Medicine, Yale School of Medicine, New Haven, CT, USA. ✉e-mail: mathieu.bakhoum@gmail.com

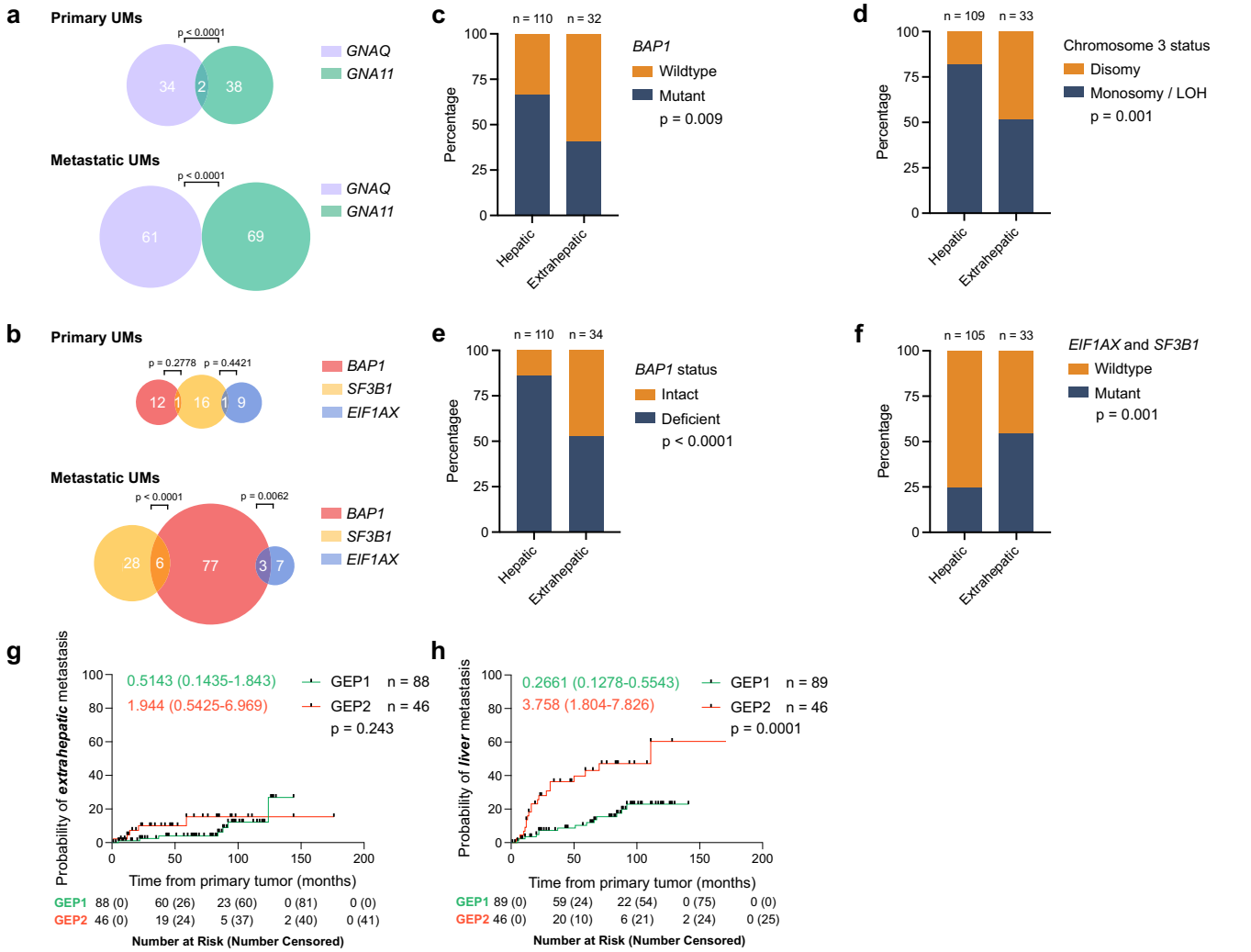

Fig. 1 | Distribution of hallmark UM mutations in primary tumors and metastases. a Proportional Venn diagram of primary UMs with *GNAQ* (purple), *GNA11* (green), *BAP1* (red), *SF3B1* (yellow), and *EIF1AX* (blue) mutations. Statistical significance of mutual exclusivity between gene pairs was determined by two-sided Fisher's exact tests. **b** Proportional Venn diagram of primary UMs with *GNAQ* (purple), *GNA11* (green), *BAP1* (red), *SF3B1* (yellow), and *EIF1AX* (blue) mutations. Proportion of **c** *BAP1* mutations (mutant shown in blue and wildtype shown in orange), **d** chromosome 3 copy number (monosomy 3 or loss of heterozygosity (LOH) shown in blue and disomy 3 shown in orange), **e** *BAP1* status (deficient (mutant or genomic copy loss) shown in blue and intact shown in orange), **f** *EIF1AX* and/or *SF3B1* mutations (mutant shown in blue and wildtype shown in orange) in hepatic and extrahepatic metastases. Statistical significance was determined using a two-sided Chi-square test. Kaplan–Meier curve showing the probability of **g** extrahepatic and **h** hepatic metastasis in patients with primary UM stratified by their bulk gene expression profile (GEP1 shown in green and GEP2 shown in red). Statistical significance was determined using the Log-rank test. Source: **a**, **b** *Yale, Karlsson* et al.[10], *Nguyen* et al.[11], *Ny* et al.[12], *Robertson* et al.[9], *and Royer-Bertrand* et al.[13];**b**–**f** *Yale, Karlsson* et al.[10], *Nguyen* et al.[11], *Ny* et al.[12], *and Royer-Bertrand* et al.[13]; **g**, **h** *Yale*.

Genotype-site associations in metastases (hepatic vs. extrahepatic)

We then examined the distribution of the hallmark prognostic mutations in hepatic versus extrahepatic metastases and found that liver metastases were enriched in *BAP1* mutations compared to extrahepatic metastases: 66.4% vs. 40.6%, respectively ($p = 0.009$) (Fig. 1c). Given the insights from TCGA data, which suggested that whole exome sequencing does not capture all *BAP1* mutations in primary UMs[9], we also assessed the prevalence of monosomy 3 in liver metastases. Of note, *BAP1* is located on chromosome 3, and primary tumors harboring *BAP1* mutations almost invariably exhibit monosomy 3. We found that 81.7% of liver metastases displayed monosomy 3 in contrast to 51.5% of extrahepatic metastases ($P = 0.001$) (Fig. 1d). Altogether, 86.4% of liver metastases were deficient in *BAP1* due to mutations or genomic copy loss, compared to 52.9% of extrahepatic metastases ($p < 0.001$) (Fig. 1e). Out of the 86 *BAP1*-mutant patients, 8.3% had single-hit *BAP1* alterations, while 91.8% had true bi-allelic loss through mutation and LOH or homozygous gene deletion (Supplementary Data 1, one patient is excluded since monosomy 3 status was not reported). Conversely, extrahepatic metastases showed an enrichment for *SF3B1* or *EIF1AX* mutations compared to liver metastases: 54.5% vs. 24.8%, respectively ($p = 0.001$) (Fig. 1f). Furthermore, we found that mutations in *GNAQ* or *GNA11* were equally prevalent in both hepatic and extrahepatic metastases (Supplementary Fig. 1a, b). Gain of chromosome 8q, associated with poorer prognosis, was not significantly enriched in hepatic or extrahepatic metastases, though additional extrahepatic specimens are warranted (Supplementary Fig. 1c). These findings suggest that hepatic metastases select for tumor clones characterized by monosomy 3, frequent *BAP1* mutations, and wildtype *EIF1AX* or *SF3B1*. This pattern implies that metastatic organotropism in UM is pre-determined by the primary tumor clones' subtypes, as identified through their hallmark mutations.

Table 1 | Patient characteristics, whole exome and whole genome data

Characteristic	
Age, median (range)	61.7 (15.9–89.0)
Sex, *n* (%)	
Male	73 (50.7)
Female	71 (49.3)
Race, *n* (%)	
White	65 (89.0)
Asian	2 (2.7)
Other	1 (1.4)
Not disclosed	5 (6.9)
Not reported in study	71
Lifetime metastasis, *n* (%)	
Hepatic only	30 (29.1)
Extrahepatic only	12 (11.7)
Hepatic and extrahepatic	61 (59.2)
Not reported in study	41
BAP1 mutation, *n* (%)	
Mutant	86 (58.7)
Wildtype	56 (39.0)
Not reported in study	2 (1.4)
Chromosome 3 status, *n* (%)	
Monosomy 3	106 (73.6)
Disomy 3	36 (25.0)
Not reported in study	2 (1.4)
EIF1AX mutation, *n* (%)	
Mutant	10 (6.9)
Wildtype	128 (88.9)
Not reported in study	6 (4.2)
SF3B1 mutation, *n* (%)	
Mutant	34 (23.6)
Wildtype	104 (72.2)
Not reported in study	6 (4.2)

Source: Yale, Karlsson et al.[10], *Nguyen* et al.[11], *Ny* et al.[12], *and Royer-Bertrand* et al.[13]

Table 2 | Patient characteristics, multivariate Cox proportional hazards regression

Characteristic	
Age, median (range)	(59.7, 15.9–89.0)
Sex, *n* (%)	
Male	36 (52.2)
Female	33 (47.8)
Race, *n* (%)	
White	60 (87.0)
Asian	2 (2.9)
Other	1 (1.4)
Refused	5 (7.3)
Not reported in study	1 (1.4)
Metastasis, *n* (%)	
Liver only	20 (29.0)
Extrahepatic only	9 (13.0)
Liver and extrahepatic	40 (58.0)
BAP1 mutation, *n* (%)	
Mutant	36 (52.2)
Wildtype	33 (47.8)
Not reported in study	0 (0)
Chromosome 3 status, *n* (%)	
Monosomy 3	43 (62.3)
Disomy 3	25 (36.2)
Not reported in study	1 (1.5)
EIF1AX mutation, *n* (%)	
Mutant	8 (11.6)
Wildtype	61 (88.4)
Not reported in study	0 (0)
SF3B1 mutation, *n* (%)	
Mutant	24 (34.8)
Wildtype	45 (65.2)
Not reported in study	0 (0)

Source: Nguyen et al.[11]

Primary tumor molecular profiling (GEP) predicts metastatic site

As an independent clinical validation of the genomic findings, we asked whether the transcriptional profiles already used in routine practice could anticipate where metastases eventually emerge. Primary UMs can be stratified into high-risk and low-risk groups based on DNA analysis or gene expression profiling (GEP). Tumors with a more favorable prognosis are typically wildtype for *BAP1*, may harbor *EIF1AX* or *SF3B1* mutations, are disomic for chromosome 3, and have a GEP1 signature. Conversely, those with worse prognosis often have *BAP1* mutations, monosomy 3, and a GEP2 signature[9,14–16]. We examined the incidence of organ-specific metastases in 135 individuals from our institution stratified by GEP classification of their primary tumor samples and with long-term follow-up data (Supplementary Table 1). Mirroring our genomic analysis, rates of extrahepatic metastasis did not differ significantly between GEP1 and GEP2 tumors ($p = 0.243$, HR = 1.94, 95% CI = 0.543–7.82) (Fig. 1g). In contrast, GEP2 UMs were far more likely to give rise to liver metastases ($p = 0.0001$, HR = 3.54, 95% CI = 1.65–7.58) (Fig. 1h). These divergent patterns strengthen the link between specific primary-tumor clones and subsequent organotropism, showing that molecular profiling at diagnosis can forecast metastatic destination and refine surveillance strategies.

BAP1 deficiency in metastases and overall survival

The enrichment of *BAP1*-deficient clones in liver lesions prompted us to examine whether these tumor-specific clones—rather than the metastatic site itself—drive survival differences after incidence of metastasis. Using clinical and genomic data from 69 patients whose metastases were analyzed using whole-exome sequencing (Table 2), we built a multivariable Cox model that included sex, age at metastasis, metastatic site (liver vs. other), and *BAP1* status in the metastatic specimen. *BAP1* loss was the dominant predictor of worse overall survival ($p = 0.0004$, HR = 4.55, 95% CI = 2.05–10.91) (Fig. 2a). In this model, neither age at metastasis nor the site of metastasis significantly influenced overall survival. Given that hepatic involvement and *BAP1* mutation are correlated, including both in the multivariable model introduces collinearity that can attenuate the coefficient for either. To isolate the prognostic contribution of the genotype, we evaluated the impact of *BAP1* mutation status on overall survival within the *liver-only* subset. In this subanalysis, *BAP1* deficiency remained associated with worse overall survival: those with *BAP1*-mutant clones had shorter survival than those with *BAP1*-intact metastases ($p = 0.018$) (Fig. 2b, and Supplementary Table 1). Median follow-up was 37.88 and 46.79 months in *BAP1* deficient an *BAP1* intact patients, respectively. Collectively, these findings suggest that, in addition to their proclivity to spread to the liver, the

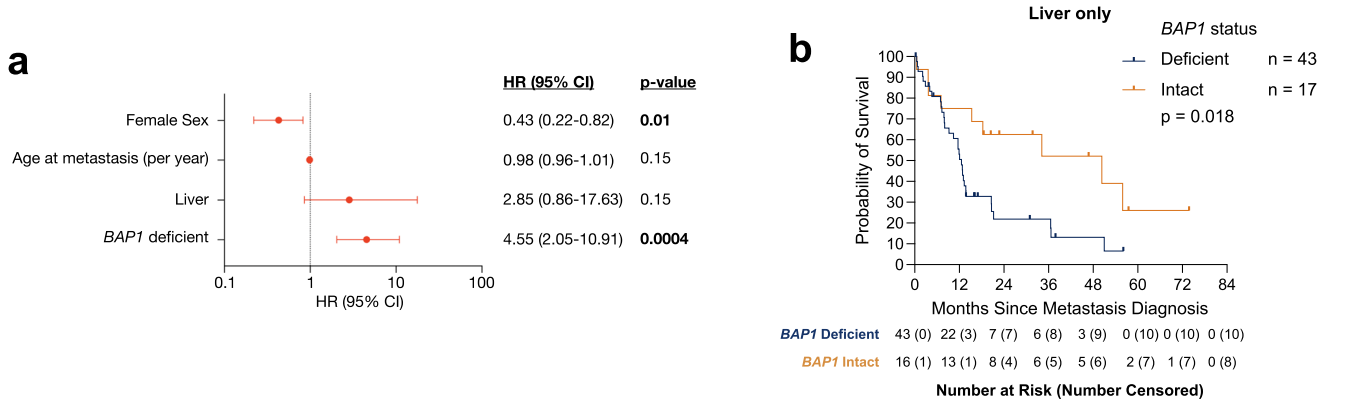

Fig. 2 | The effect of BAP1 deficiency on survival outcomes in patients with metastatic UM. a Forest plot for the multivariate Cox proportional hazards regression analysis outcomes, quantifying the impact of several prognostic variables on survival probability in patients with metastatic UM. Hazard ratios (HRs) with 95% confidence intervals (CIs) are shown. The vertical line represents a hazard ratio of 1. **b** Kaplan–Meier curve showing survival probability after liver metastasis diagnosis in patients stratified by *BAP1* status in metastases (deficient shown in blue and intact shown in orange). Statistical significance was determined using the Log-rank test. *Source:* **a**, **b** *Nguyen* et al.[11].

presence of these *BAP1* deficient clones in hepatic metastases negatively impacts survival outcomes.

Discussion

Our results demonstrate that patterns of metastatic dissemination in UM are driven by specific subtypes and genomic profiles that exist in the primary tumor. In particular, genomic profiling of hepatic and extrahepatic metastases revealed a significant relationship between *BAP1*-mutant, monosomy 3 lesions and hepatic metastasis, as well as poorer survival outcomes. Our findings are consistent with *BAP1* mutation and monosomy 3 being associated with a more aggressive, metastatic UM subtype, and *EIF1AX* and *SF3B1* mutations being associated with a more indolent subtype[7,9,17]. While the larger roles of UM hallmark mutations in the primary tumor are well-characterized, their role in determining metastasis and specifically, organotropism, are less-well understood. *BAP1* mutation and hepatic metastasis are separately well-accepted as determinants of poor prognosis, but to our knowledge, no study has directly interrogated the relationship between *BAP1* status in determining hepatic metastasis.

Our results also indicate that adverse survival outcomes are attributed to the intrinsic characteristics of specific tumor clones, beyond the involvement of the liver as a metastatic site. We have recently shown that patients with only extrahepatic metastases had a more favorable prognosis compared to those with hepatic metastases[6]. Now, we show here that these adverse survival outcomes stem from the intrinsic characteristics of specific tumors (i.e., *BAP1* deficiency), independent of the liver's involvement as a site of metastasis. Importantly, these results emphasize the need to include a comprehensive analysis of the metastatic site and genetic variability in ongoing clinical trials.

Because these high-risk *BAP1*-deficient tumors can be detected by DNA or transcriptomic profiling at diagnosis, molecular testing that is now in routine clinical use could be leveraged to stratify patients early on. Our study reveals biomarkers for hepatic and extrahepatic metastasis, which can help inform imaging schedules and identify candidates for adjuvant trials depending on a patient's primary tumor subtype.

Our study is limited by sample size and by the need to aggregate independent cohorts to assemble enough numbers of genomically profiled metastatic UM specimens. While this approach leverages rare clinical material, it introduces heterogeneity in sequencing approach. To confirm our findings, we leveraged an independent primary tumor validation cohort ($n = 135$) with molecular profiling (GEP, DecisionDx) and long-term follow up data, providing orthogonal support in line with the metastatic tissue findings. Additionally, we acknowledge that while our study demonstrates the significant association between *BAP1* status and hepatic metastasis, mechanistic studies are warranted to define how *BAP1* loss may promote hepatic tropism.

In sum, our work reveals the relationship between genomic subtypes of the primary tumor in determining hepatic metastasis and survival outcomes, which highlights the potential to predict organotropism based on routine molecular testing performed in the clinic. Our findings emphasize the need to further dissect the tumor-liver crosstalk that permits deficient *BAP1*/monosomy-3 clones to preferentially survive in the liver microenvironment.

Methods

DNA sequencing and copy number analysis

DNA sequencing data were obtained from 110 hepatic and 34 extrahepatic metastatic specimens to identify hallmark mutations of UM[10–13], and from our in-house analysis of metastasis specimens at Yale University. Specimens were collected with informed consent for research use and after obtaining approval from Yale University Institutional Review Boards. Research was conducted in accordance with the Declaration of Helsinki. Sequencing was performed with the Illumina Genome Analyzer (GA) IIx (56 tumor sample and 26 normal samples) and the Illumina HiSeq 2000 (91 tumor samples and 73 normal samples) as 75-bp paired-end reads following the manufacturer's protocols. The exome capture area comprised 22,448,951 bases in the coding regions of 15,714 genes. The sequence coverage log fold change was visualized in IGV67. The CONTRA copy number analysis program[18] was used to determine SCNAs in the matched melanoma samples. The program was run with default parameters, excluding multimapped reads. We counted the number of samples for which at least one exon in a gene had a significant CONTRA call and fitted a Poisson distribution to the resulting sample counts per gene.

We analyzed whole-*exome* sequencing data from Robertson et al.[9] and Ny et al.[12] and whole-*genome* sequencing data from Karlsson et al.[10] and Royer-Bertrand et al.[13]. Nguyen et al.[11] utilized the MSK-IMPACT targeted sequencing platform for genomic analyzes, which is a hybrid platform (exons and introns) that "identifies somatic mutations, rearrangements, and copy-number alterations in 341–468 cancer genes as well as tumor mutational burden, chromosomal instability, and microsatellite instability.

For data from Nguyen et al., we defined log2(fold change) < -0.05 as copy number loss and >0.05 as copy number gain. *BAP1* intact specimens were defined to have wildtype *BAP1* and disomy 3, while *BAP1*-deficient specimens were defined to be *BAP1* mutant and/or have monosomy 3.

We utilized two-sided Fisher's exact tests to analyze mutual exclusivity of gene pairs (e.g., *BAP1* and *EIF1AX*) in primary and metastatic UM specimens.

While a given patient may develop both hepatic and extrahepatic metastasis, we only were able to include one metastatic specimen from each patient (Yale and non-Yale cohorts), as it is very rare to have several metastases sequenced in clinical practice. Thus, hepatic and extrahepatic metastasis refers to the site of origin of the given sample, regardless of if a patient developed metastatic lesions to several organs. In order to reduce bias for including a hepatic or extrahepatic specimens, we only included studies that included hepatic and extrahepatic metastases. Of note, we chose to not include publicly available data from several other prominent UM metastasis studies due to the fact that they exclusively included hepatic metastases and no primary or extrahepatic tumors, preventing us from being able to complete the desired analyzes for the purposes of our study (PMID:31253977 and PMID:31227496). While including these studies could have even further increased our statistical significance, it would not be completely accurate given the potential batch effect in sequencing sensitivity.

Clinical data and outcomes

Given that UM sequencing and matched clinical outcome data are relatively rare compared to other cancers, it is essential to include data from previously published studies in elucidating clonal patterns of tropism, of which analysis of individual studies may not be possible otherwise, given the limited cohort size. We sought to aggregate the data from previously published cohorts, while adding our own cohort of patients from Yale New Haven Health (please see Supplementary Data 1–3 for additional information about which studies were included in each analysis; patient ages are not reported in Yale data for deidentification purposes). All statistical analyzes and graphs were generated using GraphPad Prism v9.4.1 (San Diego, California USA). Onset of metastasis Kaplan–Meier curves were generated from 135 patients with primary uveal melanoma treated at Yale New Haven Health (between March 2007 and October 2022) (Fig. 1g, h). We reviewed patients' medical charts, collecting demographic information including age, sex, race, and ethnicity, in addition to the dates and location of all metastases. The primary outcome was the probability of hepatic or extrahepatic metastasis from time of primary tumor diagnosis. Survivorship Kaplan–Meier curves were generated from Nguyen et al.[11] clinical data ($n = 69$) (Fig. 2a) The Log-rank method was used to test for significance between groups. Cox proportional hazards regression was used to control for factors (sex, age at metastasis, liver site, and *BAP1* deficiency), and hazards ratios were visualized with a Forest plot.

Data availability

Clinical data is available upon request. All patients' data analyzed from published studies are publicly available accordingly. All raw sequencing data generated for this study will be deposited to NCBI's Gene Expression Omnibus (GEO) database prior to publication. The Ny et al. 2021 data is available in the European Genome-phenome Archive (EGA) under the accession code EGAS00001005478. The Karlsson et al. 2020 data used in this study is available in EGA under the accession code EGAS00001004296. The Nguyen et al.[11] data was download from the cBioPortal study MSK-MetTropism (MSK, Cell 2021) and was filtered for patients with metastatic uveal melanoma. The TCGA Uveal melanoma data by Robertson et al.[9] was accessed through cBioPortal (Uveal Melanoma (TCGA, PanCancer Atlas))[18–25].

Received: 15 July 2025; Accepted: 7 January 2026;
Published online: 26 January 2026

References

1. Jager, M. J. et al. Uveal melanoma. *Nat. Rev. Dis. Primers* **6**, 24 (2020).
2. Gao, Y. et al. Metastasis organotropism: redefining the congenial soil. *Dev. Cell* **49**, 375–391 (2019).
3. Nguyen, D. X., Bos, P. D. & Massagué, J. Metastasis: from dissemination to organ-specific colonization. *Nat. Rev. Cancer* **9**, 274–284 (2009).
4. Collaborative Ocular Melanoma Study Group. Assessment of metastatic disease status at death in 435 patients with large choroidal melanoma in the Collaborative Ocular Melanoma Study (COMS): COMS report no. 15. *Arch. Ophthalmol.* **119**, 670–676 (2001).
5. Diener-West, M. et al. Development of metastatic disease after enrollment in the COMS trials for treatment of choroidal melanoma: Collaborative Ocular Melanoma Study Group Report No. 26. *Arch. Ophthalmol.* **123**, 1639–1643 (2005).
6. Demkowicz, P. et al. Determinants of overall survival in patients with metastatic uveal melanoma. *Cancer* **129**, 3275–3286 (2023).
7. Bakhoum, M. F. & Esmaeli, B. Molecular characteristics of uveal melanoma: Insights from the Cancer Genome Atlas (TCGA) project. *Cancers* **11**, 1061 (2019).
8. Decatur, C. L. et al. Driver mutations in uveal melanoma: Associations with gene expression profile and patient outcomes. *JAMA Ophthalmol.* **134**, 728–733 (2016).
9. Robertson, A. G. et al. Integrative analysis identifies four molecular and clinical subsets in uveal melanoma. *Cancer Cell* **32**, 204–220.e15 (2017).
10. Karlsson, J. et al. Molecular profiling of driver events in metastatic uveal melanoma. *Nat. Commun.* **11**, 1894 (2020).
11. Nguyen, B. et al. Genomic characterization of metastatic patterns from prospective clinical sequencing of 25,000 patients. *Cell* **185**, 563–575.e11 (2022).
12. Ny, L. et al. The PEMDAC phase 2 study of pembrolizumab and entinostat in patients with metastatic uveal melanoma. *Nat. Commun.* **12**, 5155 (2021).
13. Royer-Bertrand, B. et al. Comprehensive genetic landscape of uveal melanoma by whole-genome sequencing. *Am. J. Hum. Genet.* **99**, 1190–1198 (2016).
14. Tschentscher, F. et al. Tumor classification based on gene expression profiling shows that uveal melanomas with and without monosomy 3 represent two distinct entities. *Cancer Res.* **63**, 2578–2584 (2003).
15. Onken, M. D., Worley, L. A., Ehlers, J. P. & Harbour, J. W. Gene expression profiling in uveal melanoma reveals two molecular classes and predicts metastatic death. *Cancer Res.* **64**, 7205–7209 (2004).
16. Prescher, G. et al. Prognostic implications of monosomy 3 in uveal melanoma. *Lancet* **347**, 1222–1225 (1996).
17. Harbour, J. W. et al. Frequent mutation of BAP1 in metastasizing uveal melanomas. *Science* **330**, 1410–1413 (2010).
18. Hoadley, K. A. et al. Cell-of-origin patterns dominate the molecular classification of 10,000 tumors from 33 types of cancer. *Cell* **173**, 291–304.e6 (2018).
19. Ellrott, K. et al. Scalable open science approach for mutation calling of tumor exomes using multiple genomic pipelines. *Cell Syst.* **6**, 271–281.e7 (2018).
20. Taylor, A. M. et al. Genomic and functional approaches to understanding cancer aneuploidy. *Cancer Cell* **33**, 676–689.e3 (2018).
21. Liu, J. et al. An integrated TCGA Pan-Cancer Clinical Data Resource to drive high-quality survival outcome analytics. *Cell* **173**, 400–416.e11 (2018).
22. Sanchez-Vega, F. et al. Oncogenic signaling pathways in The Cancer Genome Atlas. *Cell* **173**, 321–337.e10 (2018).
23. Gao, Q. et al. Driver fusions and their implications in the development and treatment of human cancers. *Cell Rep.* **23**, 227–238.e3 (2018).
24. Ding, L. et al. Perspective on oncogenic processes at the end of the beginning of cancer genomics. *Cell* **173**, 305–320.e10 (2018).
25. Bonneville, R. et al. Landscape of microsatellite instability across 39 cancer types. *JCO Precis. Oncol.* **2017**, PO.17.00073 (2017).

Acknowledgements

We would like to acknowledge the Specimen Resource Core Yale SPORE in Skin Cancer for their samples and analysis provided for this study. M.F.B. is supported by NIH Research Grant P30CA016359 and 2P50CA121974 from the National Cancer Institute, R21EY035090 from the National Eye Institute,

by the Office of the Assistant Secretary of Defense for Health Affairs through the Melanoma Research Program under Award No. HT9425-23-1-1070, and by a grant from the Connecticut Lions Eye Research Foundation.

Author contributions

B.J. and M.F.B. designed the study. B.J., E.H., P.D., M.M., R.L., J.S., M.B., M.S., and H.K. collected and/or reviewed clinical data. A.B. and R.H. supplied tumor specimens and performed sequencing. M.F.B. supervised the project, and, together with B.J., drafted the manuscript with input from all authors.

Competing interests

The authors declare no competing interests.

Additional information

Supplementary information The online version contains supplementary material available at https://doi.org/10.1038/s41698-026-01274-8.

Correspondence and requests for materials should be addressed to Mathieu F. Bakhoum.